Notes on ecosystems stability

Onofrio Mazzarisi

August 2, 2022

1 Complexity-stability regimes

In this section we describe how the relationship between complexity and stability is shaped by dynamical properties of complex ecosystems.

Consider a competitive community of S species defined by the following dynamics for the population abundances

$$\frac{dx_i}{dt} = x_i^\alpha - x_i^\beta \sum_j A_{ij} x_j^\gamma \,, \tag{1}$$

where the sum runs from $j = 1$ to $j = S$ and the off-diagonal elements of A are extracted from a distribution with mean $\mu > 0$ and standard deviation σ while $A_{ii} = 1/K^{\beta+\gamma-\alpha}$, $\forall i$, and K is the (uniform) carrying capacity. If the equilibrium is feasible it formally reads

$$(x_i^*)^{\alpha-\beta} = \sum_j A_{ij} (x_j^*)^\gamma \,. \tag{2}$$

The element of the jacobian for $j \neq i$ read

$$J_{ij} = -\gamma x_i^\beta A_{ij} x_j^\gamma \,, \tag{3}$$

while the diagonal components read

$$J_{ii} = \alpha x_i^{\alpha-1} - \beta x_i^{\beta-1} \sum_{j\neq i} A_{ij} x_j^\gamma - (\beta+\gamma) A_{ii} x_i^{\beta+\gamma} \,. \tag{4}$$

In the case of uniform interactions ($\sigma \to 0$) the species population are all equal and the equilibrium reads

$$x^* = \left[\mu(S-1) + \frac{1}{K^{\beta+\gamma-\alpha}} \right]^{1/(\alpha-\beta-\gamma)} \,. \tag{5}$$

The jacobian evaluated at equilibrium is

$$J_{ij}\Big|_{x=x^*} = -\gamma \mu (x^*)^{\beta+\gamma-1} \,, \tag{6}$$

$$J_{ii}\Big|_{x=x^*} = \alpha (x^*)^{\alpha-1} - \beta (x^*)^{\beta+\gamma-1} \mu (S-1) - \frac{(\beta+\gamma)}{K^{\beta+\gamma-\alpha}} (x^*)^{\beta+\gamma-1} \,. \tag{7}$$

The maximum eigenvalue $\lambda_{\max}$ is $S-1$ degenerate and reads formally

$$\lambda_{\max} = J_{ii}\Big|_{x=x^*} - J_{ij}\Big|_{x=x^*} \,. \tag{8}$$

The stability condition

$$\lambda_{\max} = \alpha(x^*)^{\alpha-1} - (x^*)^{\beta+\gamma-1}\left[\beta\mu(S-1) + \frac{(\beta+\gamma)}{K^{\beta+\gamma-\alpha}} - \gamma\mu\right] < 0\,, \tag{9}$$

can be written as

$$\alpha(x^*)^{\alpha-\beta-\gamma} - \left[\beta\mu(S-1) + \frac{(\beta+\gamma)}{K^{\beta+\gamma-\alpha}} - \gamma\mu\right] < 0\,, \tag{10}$$

which, using the expression for x^* and after some manipulations reads

$$(S-1)(\beta-\alpha) > \frac{K^{\beta+\gamma-\alpha}\mu\gamma + \alpha - \beta - \gamma}{K^{\beta+\gamma-\alpha}\mu}\,. \tag{11}$$

We have then three possibilities:

$$S > 1 + \frac{K^{\beta+\gamma-\alpha}\mu\gamma + \alpha - \beta - \gamma}{K^{\beta+\gamma-\alpha}\mu(\beta-\alpha)} \qquad \text{if} \quad \alpha < \beta\,, \tag{12}$$

$$S < 1 + \frac{K^{\beta+\gamma-\alpha}\mu\gamma + \alpha - \beta - \gamma}{K^{\beta+\gamma-\alpha}\mu(\beta-\alpha)} \qquad \text{if} \quad \alpha > \beta\,, \tag{13}$$

$$\mu < \frac{1}{K^\gamma} \qquad \text{if} \quad \alpha = \beta\,. \tag{14}$$

A series of comments is in order.

- Depending on α and β we have *two regimes*: one in which increasing S enhances stability ($\alpha < \beta$) and one in which it hinders stability ($\alpha > \beta$). Notably this is independent from γ, indicating that only the interplay between the density dependence of the contribution of a species to the interactions and the density dependence of its production term that is (qualitatively) relevant; and not the form of the contribution of the competitors to the interactions.
- The critical case ($\alpha = \beta$) recovers the usual GLV result for $\gamma = 1$ and generalizes it for generic γ.
- For $K \to \infty$ and $\beta = 1 = \gamma$ we obtain

$$S = 1 + \frac{1}{1-\alpha}\,. \tag{15}$$

For symmetry reasons, it is probably sensible to consider models with $\gamma = \beta$, leaving the potential asymmetry of the competitive interaction between two species to the coefficient A_{ij}.

One can therefore identify two different regimes (complexity hinders stability (May) and complexity increases stability) characterized by the dynamical response of the population with respect to their density encoded in the exponents α and β, resepctively associated to production and losses. The GLV case $\alpha = \beta$ is right in the middle for uniform interactions ($\sigma \to 0$) and falls into the May regime otherwise ($\sigma \neq 0$).

2 On sublinear production

Observations point towards sublinear production scaling with respect to the population biomass density. This observations may refer to dynamical production or to the equilibrium production observed across a biomass gradient.

In this section we discuss how, although dynamical sublinear production does not generally leads to sublinear production across a biomass gradient, it might be necessary for sublinear scaling across a biomass gradient.

Let us focus on a single population example to calrify ideas. Consider a production function of the form

$$g(x) = rx^{\alpha}\,, \tag{16}$$

where x is the abundance of the population, $\alpha \leq 1$ specify the intensity of sublinear dynamical scaling (linear when $\alpha = 1$) and r is the parameter that allows to move across a gradient. Consider then a loss term of the form

$$l(x) = zx^{\beta}\,. \tag{17}$$

The evolution equaiton for the population is

$$\frac{dx}{dt} = g(x) - l(x) = rx^{\alpha} - zx^{\beta}\,, \tag{18}$$

which reduces to logistic growth for $\alpha = 1$ and $\beta = 2$. The equilibrium is given by

$$x^* = \left(\frac{r}{z}\right)^{1/(\beta-\alpha)}\,, \tag{19}$$

and the stability condition is given by

$$\left.\frac{d\left[g(x) - l(x)\right]}{dx}\right|_{x=x^*} < 0\,, \tag{20}$$

which leads, after some calculations, to the condition

$$\alpha < \beta\,, \tag{21}$$

independent from r and z.

The equilibrium production scales, at varying growth rate r, as $g(x^*) = z(x^*)^{\beta}$ as can be noted by Eq. (19) for r and then substituting it in the defining Eq. (16) or simply by considering the dynamical equation at stationarity. Notice that, if z is varied instead, the exponent of dynamical and across-gradient production coincide.

In summary, for an environmental change that amount to a change in r, the production across a gradient scales as $(x^*)^{\beta}$. In order for the stationary solution to be stable an exponent $\alpha < \beta$ for the dynamical produciton is needed. Therefore, in order to have sublinear $g(x^*)$ across a gradient, we need $\alpha < \beta < 1$. If the increment of the equilibrium density is due to decreasing x, equilibrium and dynamical production scale in the same way and in order to have sublinear $g(x^*)$ we need $\alpha < 1$ with $\alpha < \beta$ for stability but no constraint on β. Either way we need $\alpha < 1$.

3 Cavity solution for sublinear growth

In this section we derive the cavity solution which is used in the main text. (Refs. [1, 2, 3, 4, 5, 6])

Let us consider the dynamics of the abundances x_i of S species

$$\frac{dx_i}{dt} = r_i x_i^k - z_i x_i - x_i \sum_{j \neq i} A_{ij} x_j\,, \tag{22}$$

where the entries of the interaction matrix A_{ij} and are independently distributed with average μ and standard deviation σ and r_i and z_i are respectively growth rates extracted from distributions $P(r)$ and $P(z)$.

Let us first give an informal argument to develop intuition and show a clean connection between the initial system and the approximation obtained through the cavity method [1]. If we decompose the interaction matrix as $A_{ij} = \mu + \sigma a_{ij}$, with $a_{ij} \sim \mathcal{N}(0,1)$, the steady-state solutions x_i^* of Eq. (22) are defined by

$$0 = r_i (x_i^*)^k - x_i^* \left(z_i + \mu \sum_{j \neq i} x_j^* + \sigma \sum_{j \neq i} a_{ij} x_j^* \right) . \tag{23}$$

For large S we can write

$$\sum_{j \neq i} x_j^* \simeq S \langle x^* \rangle , \tag{24}$$

where $\langle x^* \rangle$ is the first moment of the steady state distribution, the second sum in the above equation is more problematic to simplify because in principle a_{ij} and x_j are correlated variables. The cavity method allows to rigorously and quantitatively justify the fact that, for a large community (i.e. large S) with random interactions, a single species, say x_i, does not have a strong impact on the full steady-state distribution. Therefore one does not do much wrong in considering the steady-state abundances x_j^*, for $j \neq i$, statistically independent from the paths from species i, a_{ij}. We can then invoke Central Limit Theorem (CLT) and write

$$\sum_{j \neq i} a_{ij} x_j^* \simeq \sqrt{S \langle (x^*)^2 \rangle} \eta , \tag{25}$$

η is a standard normal random variable, i.e. $\eta \sim \mathcal{N}(0,1)$. We have

$$0 = r_i (x_i^*)^k - x_i^* \left(z_i + \mu S \langle x^* \rangle + \sigma \sqrt{S \langle (x^*)^2 \rangle} \eta \right) , \tag{26}$$

which, by noticing that the species i is statistically equivalent to each other species in the community, therefore dropping the pedix, and solving for the representative abundance x^* we obtain the cavity solution

$$x^* = \left(\frac{z + \mu S \langle x^* \rangle + \sigma \sqrt{S \langle (x^*)^2 \rangle} \eta}{r} \right)^{1/(k-1)} . \tag{27}$$

Before discussing this result, let us give a slightly more formal justification. The conceptual steps in the construction of the result (see, e.g., [3]) can be stated as:

- Start with a community of $S-1$ species.
- Add a species and consider only linear response of the initial community.
- Consider non-linear feedback on the added species and find steady-state.
- Notice that each species is statistically equivalent to the added species.

[1] Notice that the simple connection we portray here is possible in the specific settings we consider but not in general, in particular the absence of correlation between off-diagonal elements of the matrix simplifies things.

Starting from Eq. (22) and using the decomposition of $A_{ij} = \mu + \sigma a_{ij}$ we can write, for large S, the steady state equation for an initial system of $S-1$ species as

$$0 = r_i (x_i^*)^k - x_i^* \left(z_i + \mu S \langle x^* \rangle + \sigma \sum_{j \neq i} a_{ij} x_j^* \right) , \tag{28}$$

with $i \in \{1, \ldots, S-1\}$. Introducing the species S causes the following change

$$0 = r_i (x_i^*)^k - x_i^* \left(z_i + \mu S \langle x^* \rangle + \sigma \sum_{j \neq i} a_{ij} x_j^* + \sigma a_{iS} x_S^* \right) , \tag{29}$$

which can be interpret as a perturbation to the mortality z_i. Defining now the susceptibilities

$$\chi_{ij} := \frac{dx_i}{dz_j} , \tag{30}$$

we can express the steady-state abundance of the species in the augmented community as a first-order Taylor expansion around the values of the one with $S-1$ species

$$x_i^* \simeq x_{i \setminus S}^* - \sigma \sum_{j=1}^{S-1} \chi_{ij} a_{jS} x_S^* , \tag{31}$$

where we now denote by $x_{i \setminus S}^*$ the steady-state abundance in the community in absence of species S. The steady-state equation for species S reads

$$0 = r_S (x_S^*)^k - x_S^* \left(z_S + \mu S \langle x^* \rangle + \sigma \sum_{i=1}^{S-1} a_{Si} x_i^* \right) , \tag{32}$$

where, using the Taylor expansion for x_i^*, the interaction term can be written as

$$\sum_{i=1}^{S-1} a_{Si} x_i^* = \sum_{i=1}^{S-1} a_{Si} x_{i \setminus S}^* - \sigma \sum_{i=1}^{S-1} \sum_{j=1}^{S-1} a_{Si} a_{jS} \chi_{ij} x_S^* . \tag{33}$$

The second term on the r.h.s. of the above equation vanishes because a_{Si} and a_{jS} are independent variables, both for $j \neq i$ and $j = i$ in our setting. The first term is a product of two independent variable and therefore, by means of CLT, we can write

$$\sum_{i=1}^{S-1} a_{Si} x_i^* \simeq \sqrt{S \langle (x^*)^2 \rangle} \eta . \tag{34}$$

Finally, considering that species S is statistically equivalent to every other species we obtain again the cavity solution (27)

$$x^* = \left(\frac{z + \mu S \langle x^* \rangle + \sigma \sqrt{S \langle (x^*)^2 \rangle} \eta}{r} \right)^{1/(k-1)} , \tag{35}$$

where $\langle x^* \rangle$ and $\langle (x^*)^2 \rangle$ are the first two moments of the abundance distribution, $\eta \sim \mathcal{N}(0,1)$ and r and z are distributed according to $P(r)$ and $P(z)$. The steady-state probability distribution

function for x^*, $P(x^*)$, can be obtained, explicitly in some cases, through the pushforward of the distribution of η, r and z and the fraction of survival species ϕ and the first two moment have can then be self-consistently computed as

$$\begin{aligned}\phi &= \int_0^\infty dx^*\ P(x^*)\,,\\ \langle x^*\rangle &= \frac{1}{\phi}\int_0^\infty dx^*\ x^* P(x^*)\,,\\ \langle (x^*)^2\rangle &= \frac{1}{\phi}\int_0^\infty dx^*\ (x^*)^2 P(x^*)\,.\end{aligned} \tag{36}$$

In the case of a unique r for every species in the community and vanishing z the distribution reads

$$P(x^*) = \frac{(1-k)|x^*|^{k-2}}{\sqrt{2\pi\sigma^2 S\langle (x^*)^2\rangle/r^2}}\exp\left\{-\frac{\left[(x^*)^{k-1}-\mu S\langle x^*\rangle/r\right]^2}{2\sigma^2 S\langle (x^*)^2\rangle/r^2}\right\}. \tag{37}$$

We can't formally solve the self-consistent equations (53) because the first and second moment of for this distribution diverges. A similiar problem is encountered in Ref. [5] in the context of consumer-resource models for the cavity calculations of the distribution of the resources which is, *mutatis mutandis*, equivalent of our case for $k = 0$.

Following [5] and assuming the fluctuations in the numerator in Eq. (27) are small, i.e. $\sigma\sqrt{S\langle (x^*)^2\rangle} \ll \mu S\langle x^*\rangle$, we Taylor expand to the first-order the cavity solution obtaining

$$x^* = \left(\frac{\mu S\langle x^*\rangle}{r}\right)^{1/(k-1)} - \frac{1}{1-k}\left(\frac{\mu S\langle x^*\rangle}{r}\right)^{(2-k)/(k-1)}\sigma\sqrt{S\langle (x^*)^2\rangle}\eta\,, \tag{38}$$

which is a gaussian variable, truncated in 0 to respect non-negativity constraint, with mean

$$\langle x^*\rangle = \left(\frac{\mu S\langle x^*\rangle}{r}\right)^{1/(k-1)}\,, \tag{39}$$

and standard deviation

$$\sqrt{\langle (x^*)^2\rangle - \langle x^*\rangle^2} = \frac{1}{1-k}\left(\frac{\mu S\langle x^*\rangle}{r}\right)^{(2-k)/(k-1)}\sigma\sqrt{S\langle (x^*)^2\rangle}\,. \tag{40}$$

In this approximation we can solve analytically the self consistency equations for the first to moment of the distribution as functions of the parameters, namely

$$\langle x^*\rangle = \left(\frac{\mu S}{r}\right)^{1/(k-2)}\,, \tag{41}$$

and

$$\langle (x^*)^2\rangle = \frac{\langle x^*\rangle^2}{\left[1-\left(\frac{1}{1-k}\right)^2\langle x^*\rangle^{2(2-k)}\sigma^2 S\right]}\,. \tag{42}$$

We can therefore use this gaussian approximation to describe the species distribution.

For practical purposes, and in order to more closely recover results from simulations we can also solve numerically the self-consistent equations (53) using a large upper cut off $x_{\rm up}$ which we checked can be widely varied and gives consistent results. In Fig. 1 we report comparisons of the cavity solution (37) obtained solving numerically the self-consistent equations and the gaussian approximation.

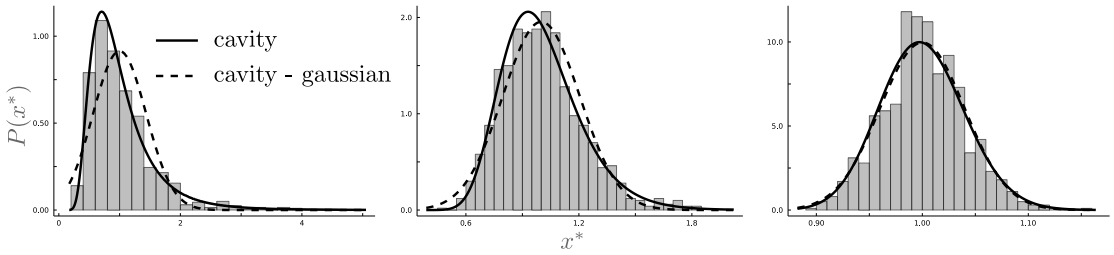

Figure 1: Cavity solution in Eq. (37) (solid line) with the moment numerically self-consistently computed using the full distribution and the gaussian approximation (dashed line) are compared with simulation for a system of $S = 10^3$ species with $r = 1$, $\mu = 10^{-3}$, $k = 3/4$ and $\sigma = \mu/10$ (left), $\sigma = \mu/20$ (center) and $\sigma = \mu/100$ (right).

3.0.1 Stability condition

Ahmadian *et al.* [**?**] consider large matrices of the form $M + LJR$, where M, L and R are deterministic matrices, and J is a random matrix with i.i.d. coefficients with zero mean and variance σ^2. Generalizing the classical 'circular law', they show that the spectrum of such matrices is contained withing the region of the complex plane defined by

$$\mathrm{Tr}[(M_\zeta M_\zeta^\dagger)^{-1}] \geq 1/\sigma^2 \quad \text{where } M_\zeta = L^{-1}(\zeta I - M)R^{-1}, \tag{43}$$

where Tr denotes the trace, dagger the Hermitian conjugate, and $\zeta \in \mathbb{C}$. In the special case where L, R and M are diagonal, this condition reduces to

$$\sum_{i=1}^{S} \frac{(L_i R_i)^2}{|\zeta - M_i|^2} \geq 1/\sigma^2 \tag{44}$$

for matrices of size S.

Following Stone [**?**], we now apply this result to generalize the stability condition to random interactions A_{ij}. From (**??**) we can write the community matrix as

$$C^* = -\mathrm{diag}(\mathbf{x}^*)[A + \mathrm{diag}(\mathbf{r}g'(\mathbf{x}^*))] \tag{45}$$

where the product of vectors is understood component-wise. Denoting $\mathbf{1}$ the rank-one matrix with all entries equal to 1, we can write $A = \mu\mathbf{1} - \mu I + J$ with J as above. For the spectral properties of interest to us, relying on rank-one perturbation theory (see Ref. [**?**]), we can consider $A = -\mu I + J$, hence C^* has the form $M + LJR$ with $L = -\mathrm{diag}(\mathbf{x}^*)$, $R = I$ and $M = \mathrm{diag}(\mathbf{x}^*)[\mu I + \mathrm{diag}(\mathbf{r}g'(\mathbf{x}^*))]$. Thus, we have that the eigenvalues of the community matrix C^* must lie within the domain

$$\sum_{i=1}^{S} \frac{(x_i^*)^2}{|\zeta - x_i^*[\mu + r_i g'(x_i^*)]|^2} \geq 1/\sigma^2. \tag{46}$$

The equation above is used in the main text to plot the spectral support of the eigenvalues in the complex plane. This domain first touches the right half-plane at $\zeta = 0$, hence stability of C^* requires

$$\sum_{i=1}^{S} [\mu + r_i g'(x_i^*)]^{-2} < \sigma^{-2}. \tag{47}$$

In the logistic model, we have $g'(x_i^*) = -1/K_i$, hence (47) becomes $\sum_i (\mu - r_i/K_i)^{-2} < \sigma^{-2}$. When growth rates and carrying capacities are all equal, this is just the May condition $\sigma\sqrt{S} + \mu < r/K$, interpreted as stating that interaction strength (μ, σ) and diversity S must be small compared to self-regulation r/K to allow for stable coexistence. In terms of scaled variables $\sigma\sqrt{S}$ and μS instability sets in for $\sigma\sqrt{S} + \mu S/S = r/K$ and in the limit of $S \to \infty$ the stability line for GLV in the scaled parameter space is given by

$$\sigma\sqrt{S} = r/K\,, \tag{48}$$

By contrast, in the sublinear model (defined by $g(x) = (x/x_0)^{k-1}$), we have $g'(x) = (k-1)x^{k-2}/x_0^{k-1}$, hence (47) reads

$$\sum_{i=1}^{S} [\mu - (1-k) r_i (x_i^*)^{k-2}/x_0^{k-1}]^{-2} < \sigma^{-2}\,. \tag{49}$$

Making use of the cavity solution $P(x^*)$ obtained in sec. **??** for equal r for every species and vanishing z, we can write this condition as

$$S \int dx^*\ P(x^*)[\mu - (1-k) r (x^*)^{k-2}/x_0^{k-1}]^{-2} < \sigma^{-2}\,. \tag{50}$$

The stability line in the scaled parameter space can be obtained from the above expression

$$\sigma\sqrt{S} = \left\{ \int dx^*\ P(x^*)[\mu S/S - (1-k) r (x^*)^{k-2}/x_0^{k-1}]^{-2} \right\}^{-1/2}\,. \tag{51}$$

In the limit $S \to \infty$ and noticing that $P(x^*)$ depend on S only through $\sigma\sqrt{S}$ and μS we finally obtain

$$\sigma\sqrt{S} = \left\{ \int dx^*\ P(x^*)[(1-k) r (x^*)^{k-2}/x_0^{k-1}]^{-2} \right\}^{-1/2}\,. \tag{52}$$

In order to obtain the stability line we solve, for a given S and given μ, the set of self-consistency equations plus the stability condition numerically, either by using the full cavity solution, Eq. (37), or the gaussian approximation using the moments in Eq. (41) and Eq. (42)

$$\begin{aligned}
\phi &= \int_0^\infty dx^*\ P(x^*)\,, \\
\langle x^* \rangle &= \frac{1}{\phi} \int_0^\infty dx^*\ x^* P(x^*)\,, \\
\langle (x^*)^2 \rangle &= \frac{1}{\phi} \int_0^\infty dx^*\ (x^*)^2 P(x^*)\,, \\
\sigma\sqrt{S} &= \left\{ \frac{1}{\phi} \int_0^\infty dx^*\ P(x^*)[(1-k) r (x^*)^{k-2}/x_0^{k-1}]^{-2} \right\}^{-1/2}\,.
\end{aligned} \tag{53}$$

The results are plotted in Fig. 2.

3.0.2 Extinction condition

In this section we derive an expression to estimate the extinction threshold in parameter space. It can be obtained by means of the gaussian approximation of the cavity solution.

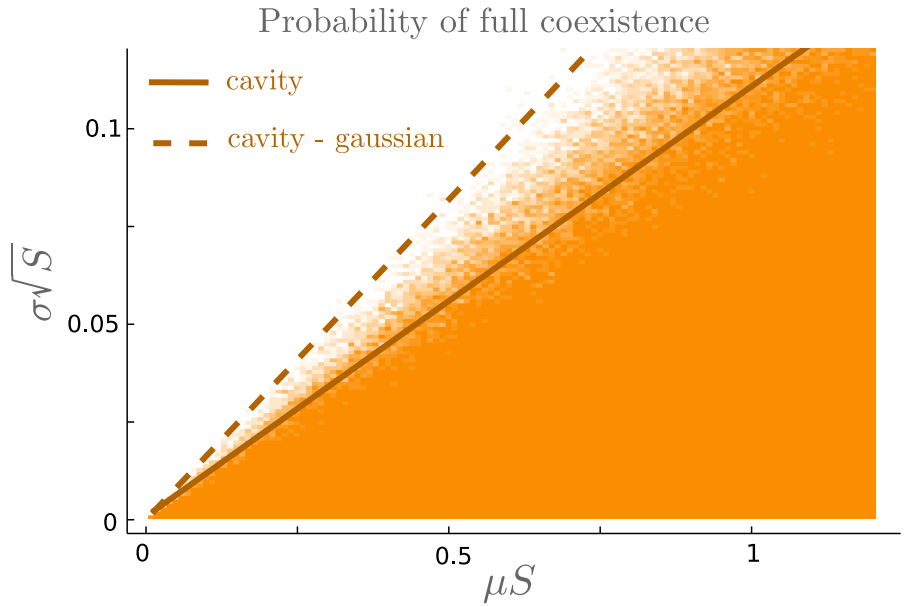

Figure 2: Simulation showing probability of full coexistence, (from dark orange (probability 1) to white (probability 0)) compared with analytical estimation of the stability threshold (solid line obtained using the full cavity solution and the dashed line using the gaussian approximation). The number of species is kept fixed to $S = 100$ and μ and σ are varied.

We recall the definition for the first and second moment of the distribution of x

$$\langle x^* \rangle = \left(\frac{\mu S}{r x_0^{1-k}} \right)^{1/(k-2)} , \tag{54}$$

and

$$\langle (x^*)^2 \rangle = \frac{\langle x^* \rangle^2}{\left[1 - \left(\frac{1}{1-k} \right)^2 \langle x^* \rangle^{2(2-k)} \sigma^2 S \right]} , \tag{55}$$

where we explicitely wrote down the scale x_0 because in the following we want to study both, the case where the growth term is not modified below threshold and when is set equal to zero causing every species below threshold to go extinct.

First we approximate the second moment by expanding it to the first order in the second addend in the denominator

$$\langle (x^*)^2 \rangle \approx \langle x^* \rangle^2 + \left(\frac{1}{1-k} \right)^2 \langle x^* \rangle^{2(3-k)} \sigma^2 S , \tag{56}$$

so that the standard deviation can be written as

$$\sqrt{\langle (x^*)^2 \rangle - \langle x^* \rangle^2} \equiv \mathrm{std}(x^*) = \left(\frac{1}{1-k} \right) \langle x^* \rangle^{(3-k)} \sigma \sqrt{S} . \tag{57}$$

Now we want to write down the condition under which the average minus a number ν of standard deviations touches zero, or x_0 if the threshold is enforced. Let us consider this latter

more general case first. The condition reads

$$\langle x^* \rangle - \nu \, \mathrm{std}(x^*) = x_0 \,, \tag{58}$$

which, using Eq. (57), becomes

$$\langle x^* \rangle - \nu \left(\frac{1}{1-k} \right) \langle x^* \rangle^{(3-k)} \sigma \sqrt{S} = x_0 \,. \tag{59}$$

Substituting the expression for the average and solving for $\sigma\sqrt{S}$, we finally obtain

$$\sigma\sqrt{S} = \frac{1-k}{\nu} \left[\left(\frac{\mu S}{r x_0^{1-k}} \right) - x_0 \left(\frac{\mu S}{r x_0^{1-k}} \right)^{(k-3)/(k-2)} \right] , \tag{60}$$

which reduces in the case where no condition is imposed in x_0 to the linear relation between the scaled parameters $\sigma\sqrt{S}$ and μS

$$\sigma\sqrt{S} = \left(\frac{1-k}{\nu r x_0^{1-k}} \right) \mu S \,. \tag{61}$$

In order to avoid arbitrariness in the choice of ν we can estimate an S dependent value which accounts for the fact that the same equilibrium distribution but with more species (therefore the same point in the $\sigma\sqrt{S} - \mu S$ plane for higher S) implies a smaller sample minimum. One way to make analytical progress is to find the value $x_{\min}$ for which the gaussian approximation for the distribution touches $1/S$. There will be two points satisfying this conditions and we are interested in the lower one. The rationale behind this is that in a community of S species, less then one, on average, will be below $x_{\min}$. We have

$$\frac{1}{\sqrt{2\pi \mathrm{std}(x^*)^2}} \exp \left[- \frac{(x_{\min} - \langle x^* \rangle)^2}{2\mathrm{std}(x^*)^2} \right] = \frac{1}{S} \,, \tag{62}$$

which, solving for $x_{\min}$, gives

$$x_{\min} = \langle x^* \rangle - \mathrm{std}(x^*) \sqrt{2 \ln \left(\frac{S}{\sqrt{2\pi \mathrm{std}(x^*)^2}} \right)} \,. \tag{63}$$

For large S we can approximate the last equation by

$$x_{\min} = \langle x^* \rangle - \sqrt{2 \ln S} \; \mathrm{std}(x^*) \,, \tag{64}$$

from which we can read out our estimate for ν, comparing with Eq. (58), i.e.

$$\nu = \sqrt{2 \ln S} \,. \tag{65}$$

In Fig. (3) the extinction threshold is plotted against simulations for the case where no condition is imposed at the threshold x_0 and the case where growth is set to zero below the threshold.

The same arguments apply to GLV, which, we recall, describes S species evolving as

$$\frac{dx_i}{dt} = r x_i (1 - \frac{x_i}{K}) - x_i \sum_{j \neq i} A_{ij} x_j \tag{66}$$

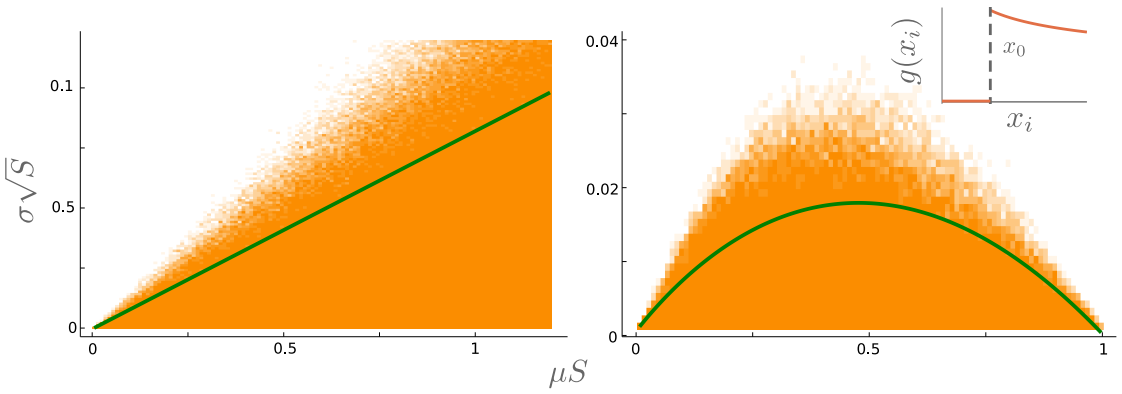

Figure 3: Simulation showing probability of full coexistence, (from dark orange (probability 1) to white (probability 0)) compared with analytical estimation of the extinction threshold (green lines). In both panels the number of species is kept fixed to $S = 100$ and μ and σ are varied, the left panel shows results for the case in which no threshold effect is enforced while the right panel report the case where growth is set to zero if the population of a species touches the threshold. The analytical lines are plotted from Eq. (61) (left) and Eq. (60) (right) both with $\nu = \sqrt{2 \ln S}$.

with A_{ij} distributed with mean μ and standard deviation σ and we assume here r and K equal for all species, allowing to estimate the extinction threshold also in this case.

The equilibrium distribution obtained through the cavity method is a truncated gaussian [REFS] with average

$$\langle x^* \rangle = \frac{K}{1 + K\mu S/r}\,, \tag{67}$$

and standard deviation, written as a function of the average,

$$\mathrm{std}(x^*) = \frac{\sigma\sqrt{S} K \langle x^* \rangle}{\sqrt{1 - \frac{K^2\sigma^2 S}{r^2}}}\,, \tag{68}$$

plugging in the last two equations in the extinction threshold condition (58), for $x_0 = 0$ leads to

$$\sigma\sqrt{S} = \frac{r}{K\sqrt{\nu^2 + 1}}\,, \tag{69}$$

which is an horizontal line in the parameter space lower then the stability condition $\sigma\sqrt{S}$ and recovers it for $\nu = 0$.

4 Model connection with data on productivity

Our model is informed by macroecological observations of biomass density production across major groups. In this section we attempt a closer connection to the data.

We define our model in the following way

$$\frac{db_i}{dt} = \underbrace{r_i b_i \left(\frac{b_i}{b_0}\right)^{k-1} \theta(b_i - b_0)}_{\text{Production}} - \underbrace{b_i \sum_{j \neq i} A_{ij} b_j}_{\text{Losses}}\,, \tag{70}$$

where $k < 1$ specify the intensity of sublinear dynamical scaling, the entries of the interaction matrix A_{ij} are randomly distributed with average μ and standard deviation σ, the r_i are growth rates extracted from a distribution $P(r)$, the biomass density scale b_0. For the sake of clarity let us summarize the dimensionality of the several terms involved in the model

$$[b_i] = [b_0] = \frac{\text{mass}}{\text{area}} \ , \quad [r_i] = \frac{1}{\text{time}} \ , \quad [A_{ij}] = \frac{\text{area}}{\text{mass} \times \text{time}} \ . \tag{71}$$

The density biomass scale b_0 set the value at which the per capita growth rate is r_i. When we want to consider this value the maximum per capita growth rate for a given species we can consider b_0 as the minimal biomass density for a given species at which it is able to reproduce. In this case we can impose that there is no growth for $b_i < b_0$ through a Heaviside function $\theta(b_i - b_0)$.

Next we connect the model with the average body mass m of a community. The time scale of the problem are widely observed [7] to scale with the body mass with an exponent $-1/4$. Therefore we assume that the average growth rate $\langle r \rangle$ for a community and the average interaction μ scale with the average body mass of the community to the $-1/4$, i.e. $\langle r \rangle \sim m^{-1/4}$ and $\langle \mu \rangle \sim m^{-1/4}$. We have no reasons to assume a systematic variation of the ratio μ/σ with respect to the mass. We assume for simplicity that b_0 is species and mass independent. We may invoke an ecological argument to justify this assumption, indeed the observed biomass densities across major group have a mass independent lower bound (within two or three order of magnitude compared with the astronomical difference of nearly 20 order of magnitude in body mass). The population density scale for a given community of average mass m, $n_0 := (b_0)/m$, is then assumed to be inversely proportional to the mass.

To compare this data with outcomes of the model we proceede as follows. We characterize a community type by an average mass, and therefore by an average growth rate $\langle r \rangle$, then we solve the model for different communities with same average r but different μ and plot the resulting $\langle b^* \ g(b^*) \rangle$ vs $\langle b^* \rangle$. In this process we keep the coefficient of variation σ/μ constant. We keep S constant and vary μ in a range which scales with m in the same way that the average r does across community type: within a community type we plot results for communities with $\mu S \in (\langle r \rangle \mu_{\min}, \langle r \rangle \mu_{\max})$, with $\mu_{\min}$ and $\mu_{\max}$ possibly mass dependent but with $\mu_{\min} < 1$ and $\mu_{\max} > 1$. In other words, in order to not introduce strong biases towards specific masses, within community type and for every community type, we simulate different environment going from a μ which is less than $\langle r \rangle$ to one which is more than $\langle r \rangle$. We can summarize the assumptions in the following way.

Assumptions

- b_0 is body mass independent and n_0 for a community is inversely proportional to the average body mass m of the community.
- $r \sim m^{-1/4}$ and characterize the typical growth rate of a community type with the typical body mass m.
- $\mu \sim m^{-1/4}$ for a given community type of average mass m.
- To explore ecological variation among communities of the same type we cosider different $\mu S \in (r\mu_{\min}, r\mu_{\max})$ with $\mu_{\min} < 1$ and $\mu_{\max} > 1$.
- the coefficient of variation μ/σ does not vary systematically both within and across community type.

- $k < 1$, in particular, in orderd to closely recover the observed pattern, $k \simeq 3/4$

Each point in Fig. 4 correspond to an entire community, with on the x axis the average biomass of the community $\langle b^* \rangle$ and on the y axis the average equilibrium production of the community $\langle b^*\ g(b^*) \rangle$. Within each community type the points follow a scaling law with exponent aroun 3/4.

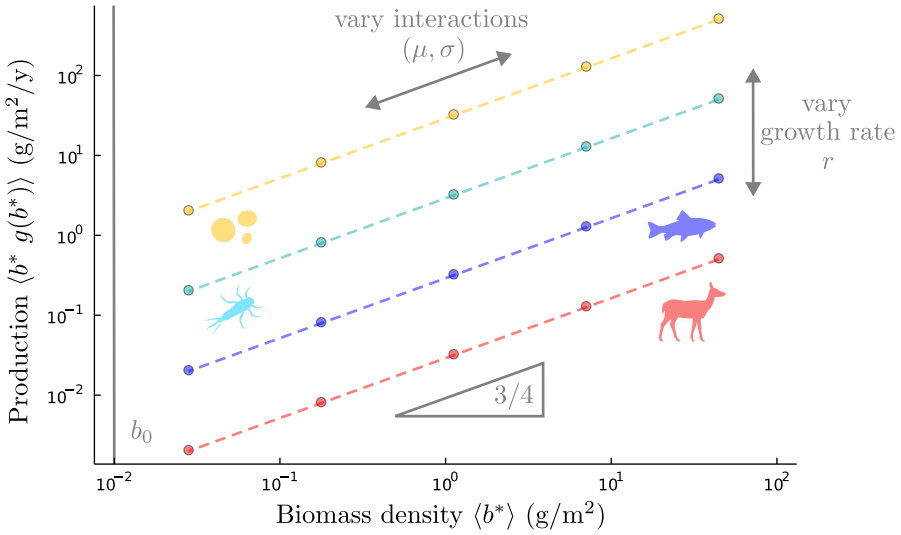

Figure 4: Make figure with precise values of r Average equilibrium production $\langle b^*\ g(b^*) \rangle$ plotted versus average equilibrium biomass density $\langle b^* \rangle$. Each dot represents simulations for a community of $S = 50$ species, each color correspond to a specific growth rate value: $r = 10^2$ yellow, $r = 10$ light blue, $r = 1$ blue and $r = 10^{-1}$ red with the dimension of 1/y. The exponent in the growht rate is set as $k = 3/4$ and the biomass scale is $b_0 = 10^{-2}$ (g/m^2), the different points within a color (i.e. same r) correspond to $\mu S \in \{r10^2, r10, r, r^10^{-1}, r10^{-2}\}$. We set everywhere the coefficient of variation $\sigma/\mu = 0.7$. The dashed lines represent theoretical predictions from the cavity solution.

4.1 Analytical prediction of average equilibrium production

In order to compute how the average production changes with respect to the average biomass density in our context we can resosrt to the cavity solution computed in the previous section which *mutatis mutandis* in terms of biomass density reads

$$b^* = \left(\frac{\mu S \langle b^* \rangle + \sigma \sqrt{S \langle (b^*)^2 \rangle} \eta}{r\ b_0^{1-k}} \right)^{1/(k-1)} . \tag{72}$$

At equilibrium we have

$$b^* g(b^*) \equiv \underbrace{r b^* \left(\frac{b^*}{b_0} \right)^{k-1}}_{\text{Production}} = \underbrace{b^* (\mu S \langle b^* \rangle + \sigma \sqrt{S \langle (b^*)^2 \rangle} \eta)}_{\text{Losses}} , \tag{73}$$

therefore

$$\langle b^* g(b^*) \rangle = \mu S \langle b^* \rangle^2 + \sigma \sqrt{S \langle (b^*)^2 \rangle} \langle b^* \eta \rangle . \tag{74}$$

Invoking the gaussian approximation we know that the average reads

$$\langle b^* \rangle = \left(\frac{\mu S}{r\ b_0^{1-k}} \right)^{1/(k-2)} , \tag{75}$$

which, if inverted for μS, gives

$$\mu S = r\ b_0^{1-k} \langle b^* \rangle^{k-2} , \tag{76}$$

which imply that the first term on the r.h.s. of Eq. (74) is equal to $r\ b_0^{1-k} \langle b^* \rangle^k$.

The second term is more involved. By writing explicitely the expression for b^* it reads

$$\begin{aligned} \sigma \sqrt{S\langle (b^*)^2 \rangle} \langle b^* \eta \rangle &= \sigma \sqrt{S\langle (b^*)^2 \rangle} \left\langle \left(\frac{\mu S \langle b^* \rangle + \sigma \sqrt{S\langle (b^*)^2 \rangle} \eta}{r\ b_0^{1-k}} \right)^{1/(k-1)} \eta \right\rangle , \\ &= \sigma \sqrt{S\langle (b^*)^2 \rangle} r^{1/(1-k)} b_0 \left\langle \frac{\eta}{(\mu S \langle b^* \rangle + \sigma \sqrt{S\langle (b^*)^2 \rangle} \eta)^{1/(1-k)}} \right\rangle . \end{aligned} \tag{77}$$

The leading term in the denominator for large S is $(\mu S \langle b^* \rangle)^{1/(1-k)}$, which for $k = 3/4$ is proportional to S^4, while the others have a lower order dependence on S. Therefore if we approximate the whole denominator by $(\mu S \langle b^* \rangle)^{1/(1-k)}$ and recall that $\langle \eta \rangle = 0$ we can neglect this term and approximate the average production as

$$\langle b^* g(b^*) \rangle \simeq r\ b_0^{1-k} \langle b^* \rangle^k . \tag{78}$$

4.2 Note on the origin of sublinear growth

Mechanistic justifications of the emergence of sublinear dynamical growth at the coarse level of description of the model studied in this work should be sought after. However our results suggest that mechanistic descriptions of community dynamics leading to an effective sublinear growth (or, more generally, to a relative change of production with respect of population abundance lower than the relative change of losses, see Sec. 1) will be qualitatively characterized by a positive correlation beteween stability and complexity.

The macroecological data which inspired the model studied in this work have mixed origin, some can be directely connected with dynamical production and other are cross-ecosystem patterns. More precise and systematic observations of the former and validation of the latter at the ecosystem level with temporal data are needed (see Ref. [8] for an example of a macroecologially motivated model and subsequent discussion about within ecosystem validation).

Among the task that future theoretical work should aim at, we suggest

- Building a mechanistic understanding of the emergence of sublinear dynamical scaling from realistic models.
- Connecting the abundance prediction from community models with macroecological patterns related to abundance. In particular when we go from within community description to cross-community.
- Exploring in detail possibilities different from sublinear dynamical scaling to explain cross-ecosystem sublinear scaling and test indipendent predicrtions.

Future urgent experimental and field research include

- Collecting temporal data within ecosystems and devise ways to estimate the population abundance or density dependence on production.
- Extending the spectrum of data available in order to further validate the evidence of sub-linear production.

5 Macroecological laws

In this section we compare macroecological patterns with prediction of our model specifying in which way we construct the observable to compare and under which assumptions in addtion to the ones described in the construction of the model.

5.1 Species abundance distribution

The species abundance distribution distribution within a community is often well fitted by a log-normal distribution. In order to recover this pattern for the abundance density n_i with our model we assume that the growth rates r_i follows a log-normal distribution.

Assumptions

- $\ln r \sim \mathcal{N}(\mu_r, \sigma_r)$.

Predictions

- We predict that n^* roughly follows a log-normal distribution as well and, if we consider $k = 3/4$, it has shape parameter 4 times larger than the one for r.

We can work out an exact calculation in the case of uniform interactions (i.e. $\sigma \to 0$), which works well also for small but finite σ. In this case the cavity solution for n^* (Eq. (27)) reads

$$n^* = \left(\frac{\mu S \langle n^* \rangle}{r \; n_0^{1-k}} \right)^{1/(k-1)} , \tag{79}$$

where we recall that consider for simplicity that the scale n_0 is the same for all the species in the community and set it to unity, $n_0 = 1$, in the following.

We can obtain the probability distribution for n^* by pushing forward the one for r, $P(n^*) = P(r(n^*))|dr/dn^*|$. Given that $r(n^*)$ reads

$$r = \frac{(n^*)^{k-1}}{\mu S \langle n^* \rangle} , \tag{80}$$

and

$$\left| \frac{dr}{dn^*} \right| = \frac{(1-k)(n^*)^{k-2}}{\mu S \langle n^* \rangle} , \tag{81}$$

we obtain that n^* is as well a log-normal random variable

$$\ln n^* \sim \mathcal{N}(\mu_{n^*}, \sigma_{n^*}) , \tag{82}$$

with

$$\mu_{n^*} = \frac{\mu_r - \ln(\mu S \langle n^* \rangle)}{(1-k)} , \tag{83}$$

$$\sigma_{n^*} = \frac{\sigma_r}{(1-k)} . \tag{84}$$

Notice that the scale parameter is amplified by a factor $1/(1-k)$, which in the case of $k \simeq 3/4$ correspond to a species abundance distribution four times wider than the growth rate distribution.

In this case we only need to solve a self-consistent equation for the average $\langle n^* \rangle$ to complete the cavity solution. This can be done analytically because the expression of the average for a log-normal distribution is known

$$\langle n^* \rangle = \exp\left(\mu_{n^*} + \frac{\sigma^2_{n^*}}{2}\right), \tag{85}$$

and we have

$$\langle n^* \rangle = (\mu S)^{(k-2)} \exp\left[\frac{2\mu_r(1-k) + \sigma_r^2}{2(1-k)(2-k)}\right]. \tag{86}$$

In Fig. 5 the cavity results are compared with simulations showing perfect agreement in the case $\sigma \to 0$ (left panel) and good agreement also in the case of finite σ (right panel).

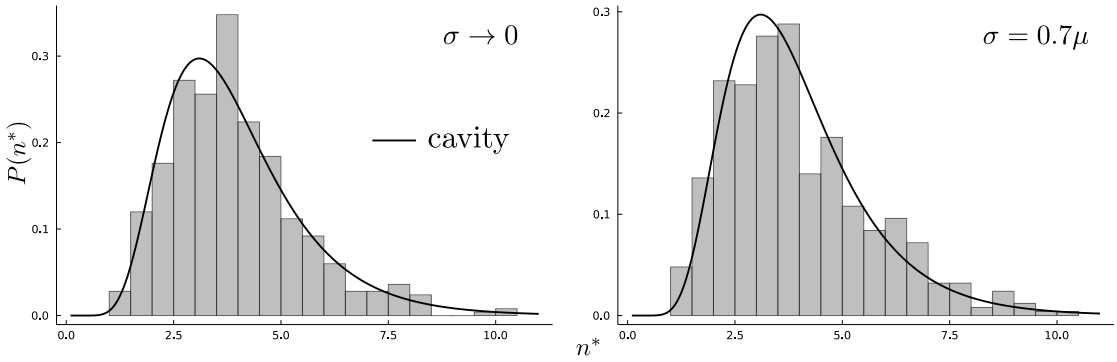

Figure 5: Cavity solution compared to simulations for log-normal distribution of growth rates r, $\ln P(r) = \mathcal{N}(\mu_r, \sigma_r)$, with $\mu_r = 1$ and $\sigma_r = 1/10$ and a pool of $S = 500$ species with $\mu = 10^{-3}$, $k = 3/4$ and $\sigma \to 0$ (left panel) while $\sigma = 0.7\mu$ (right panel).

In Fig. 6 we report the abundance distributions for the four community types as parametrized in the model construction (details in caption).

5.2 Mean-variance scaling

The variance of fluctuations in biomass densities for time series of different species scale with mean biomass density with an exponent from 3/2 to 2. We consider again a log-normal distribution for r and that the loss term of our model exhibits variation in mortality (e.g. μ varies).

Assumptions

- $\ln r \sim \mathcal{N}(\mu_r, \sigma_r)$ (only needed for analytical results).
- μ varies (in the case of uniform r, the ratio μ/σ should be constant).

Predictions

- Taylor's law.

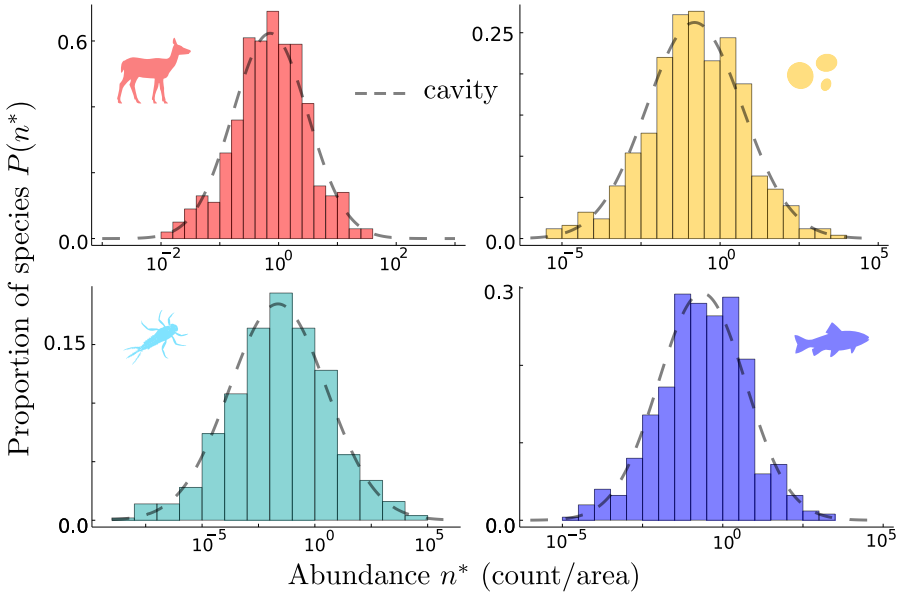

Figure 6: Abundance distribution of species resulting from the dynamics for the four community types as parametrized in the model construction see (Fig. 4), but with $S = 500$ species to obtain better statistics. In particular, in every panels, we set $\mu S = \langle r \rangle$ and $\sigma/\mu = 0.7$ and r is lognormally distributed with mode chose as $\exp(\mu_r) = \langle r \rangle B_0^{1-k}$ specific for each color as per model construction and shape parameter $\sigma_r = 0.16$ for red, 0.38 for blue, 0.54 for light blue and 0.34 for yellow. The dashed lines correspond to the cavity solution in Eq. (82) which well compare with simulations.

We consider again the cavity result in the limit $\sigma \to 0$ which, in the case of $\ln r \sim \mathcal{N}(\mu_r, \sigma_r)$, gives $\ln b^* \sim \mathcal{N}(\mu_{b^*}, \sigma_{b^*})$ with

$$\mu_{b^*} = \frac{\mu_r - \ln(\mu S \langle b^* \rangle)}{(1-k)}, \tag{87}$$

$$\sigma_{b^*} = \frac{\sigma_r}{(1-k)}. \tag{88}$$

By varying μ only the scale parameter μ_{b^*} is modified. Therefore if we consider the mean and variace of the log-normal distribution

$$\langle b^* \rangle = \exp\left(\mu_{b^*} + \frac{\sigma_{b^*}^2}{2}\right), \tag{89}$$

$$\mathrm{var}(b^*) = \left(\exp[\sigma_{b^*}^2] - 1\right) \exp\left(2\mu_{b^*} + \sigma_{b^*}^2\right), \tag{90}$$

$$\tag{91}$$

it is straightforward to realize that the mean is proportional to $\exp(\mu_{b^*})$, while the variance to $\exp(2\mu_{b^*})$, therefore

$$\mathrm{var}(b^*) \propto \langle b^* \rangle^2, \tag{92}$$

i.e., Taylor's law. In Fig. 7 we report a comparison with simulations with lognormally distributed r and $\sigma \to 0$, lognormally distribute r and finite $\sigma = \mu/10$, to show that the results hold in this

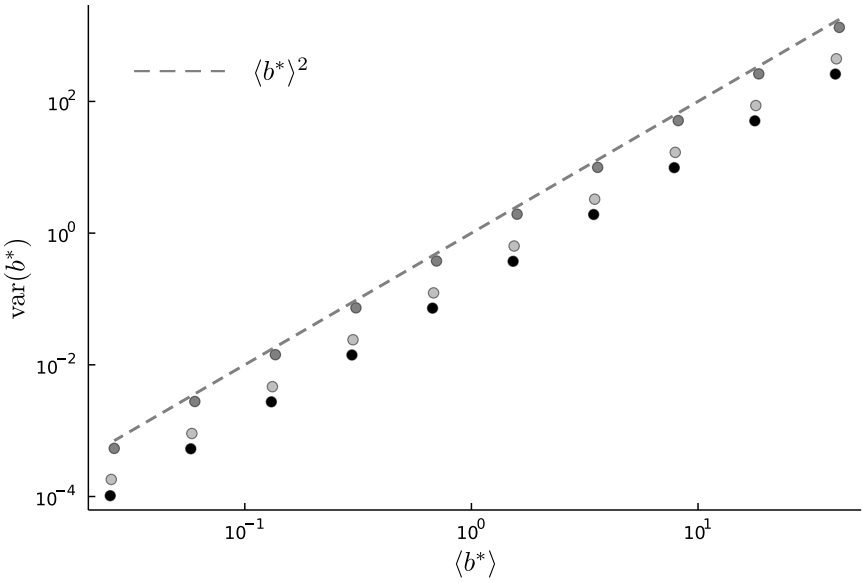

Figure 7: Variance of the species biomass density distribution plotted against the mean, each dot is a community with a specific $\mu \in \{\langle r \rangle 10^{-2}, \langle r \rangle 10^2\}$, whith $S = 10^3$, $k = 3/4$ and black dots correspond to $\ln P(r) = \mathcal{N}(\mu_r, \sigma_r)$, with $\mu_r = 1$, $\sigma_r = 1/10$ and $\sigma \to 0$, dark gray to $\sigma = \mu/10$ with the same distribution for r and light gray dots correspond to uniform $r = 1$ and $\sigma = \mu/10$.

case, and, even if in this case we don't have analytical results (I manage to obtain one, to be added), also with uniform $r = 1$ and finite $\sigma = \mu/10$.

In Fig. 8 we report variance vs. average for the communitites parametrized as in model construction (Fig. 4), finding a good agreement with Taylor's law, see caption for details.

5.3 Size-density scaling

The species-level relation of population density vs. body mass is nearly inversely proportional across major groups. By relying on no further assumptions then in those used to connect the model with data on production we predict a size-density scaling with exponent -1.

Assumptions

- Same as for the connection of the model with data on production.

Predictions

- Size-density scaling with exponent -1.

We start from the cavity solution for the equilibrium biomass density b_0

$$b^* = \left(\frac{\mu S \langle b^* \rangle + \sigma \sqrt{S \langle (b^*)^2 \rangle} \eta}{r \; b_0^{1-k}} \right)^{1/(k-1)} , \tag{93}$$

where we consider r uniform and different for each community type as in the model connection with data on production. Each community is characterized by an average mass m, and, given that we consider $\mu S \propto r$ (it varies in a range of two order of magnitude above and below r), it

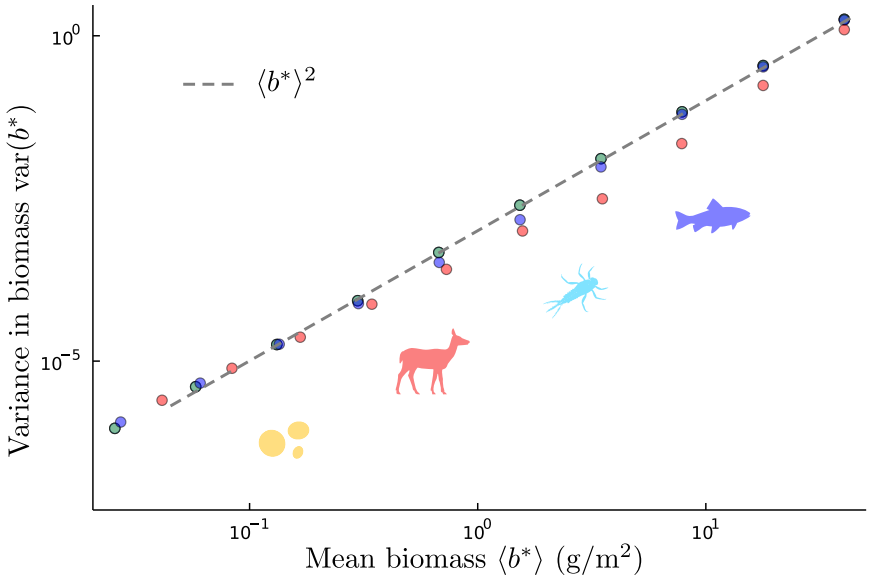

Figure 8: Make figure with precise values of r Variance of the species biomass density distribution plotted against the mean, each dot is a community is parametrized as in the model construction (see caption of Fig. 4).

cancels out with r leaving no mass dependence. Therefore the average numerical densities $\langle n^* \rangle$ of different community types will be inversely proportional to their mass m with a spread on the y axes due to different (μ, σ)

$$\langle n^* \rangle \sim m^{-1} \,. \tag{94}$$

In Fig. 9 we report the average numerical density vs. body mass for the different community types using the same parameters from Fig. 4.

6 Macroecology with GLV

In this section we discuss how to reproduce the production data wiht the GLV model and under what assumption it recovers the macroecological pattern discussed in the paper.

Let us recall the GLV model to describe the biomass density of S species

$$\frac{dB_i}{dt} = r_i B_i \left(1 - \frac{B_i}{K_i}\right) - \sum_{j \neq i} A_{ij} B_j \,, \tag{95}$$

where A_{ij} are distributed with mean μ and standard deviation σ, K_i are the carrying capicties and we redefine the growth rates r_i as the difference between growht and mortality rate defined before, i.e. $\bar{r}_i := r_i - z_i$ and we drop the bar. The cavity solution for this system reads [1]

$$B^* = K \left(1 - \frac{\mu S \langle B^* \rangle + \sigma \sqrt{S \langle (B^*)^2 \rangle}}{r}\right) \,, \tag{96}$$

with r and K in general distributed as $P(r)$ and $P(K)$ respectively.

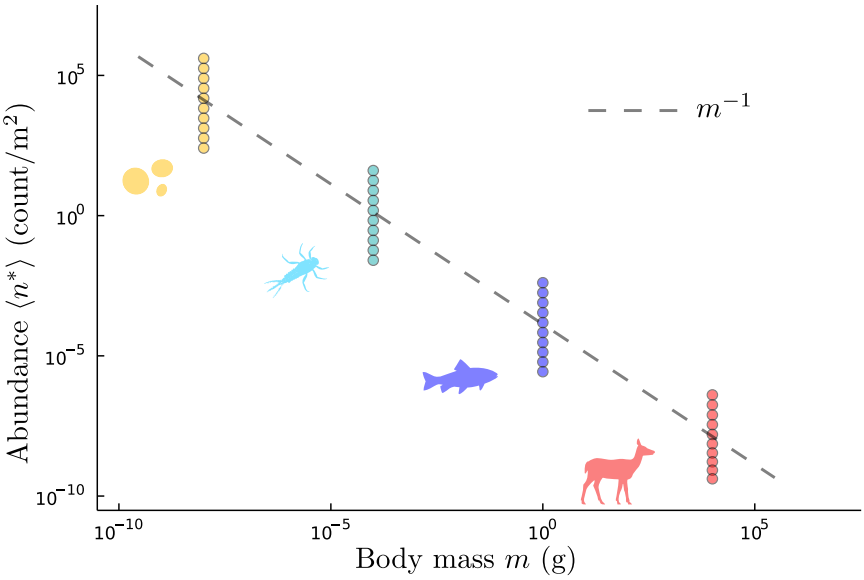

Figure 9: Make figure with precise values of r Numerical density distribution vs. body mass for each community type parametrized as in the model construction (Fig. 4).

Let us work in the case in which r and K are the same for every speceis and we assume $\sigma \to 0$ for simplicity to discuss the assumption needed to obtain the production scaling. In this case each species in the community has the same biomass density

$$B^* = \frac{K}{1 + \mu S K/r}\,, \tag{97}$$

which recovers $B^* = K$ for vanishing inter-species interactions.

We will assume that intra-specific and inter-specific interactions scale in the same way $\mu = ar/K$ (with $a < 1$ to guarantee sabitlity). Notice that for $a \simeq 1$, for large S, we can write $B^* \simeq K/S$, which allows for an intrepretation of K as a community parameter, a global carrying capacity, which encode the maximum biomass density that a specific ecosystem can sustain. In the following we arbitrarly set $a = 1/S$ in order to have good stability properties, in this case $B^* = K/2$.

6.1 Production-biomass scaling

The key assumption we need to connect with sublinear proiduciton-biomass scaling is that the growth rate r should scale with the carrying capacity as $r = bK^{k-1}$. The production, using the solution for B^* and our assumptions reads then

$$rB^*\left(1 - \frac{B^*}{K}\right) = \frac{b}{2^{2-k}}(B^*)^k\,. \tag{98}$$

As we show in Fig. 10 this result holds also for finite σ (we set $\sigma = \mu$).

In order to reproduce the data, we set for each community b as the difference of the representative growth rates and mortalities discussed in the main text, namely 0.37 for mammal,

7.05 for fish, 30 for invertebrate and 437 for protists. Then a variation of 4 order of magnitude for K is consistent with 1 order of magnitude variation around these values for the effective growth rates. In Fig. 10 we report comparisons of simulations with analytical prediction of the produciton-biomass scaling.

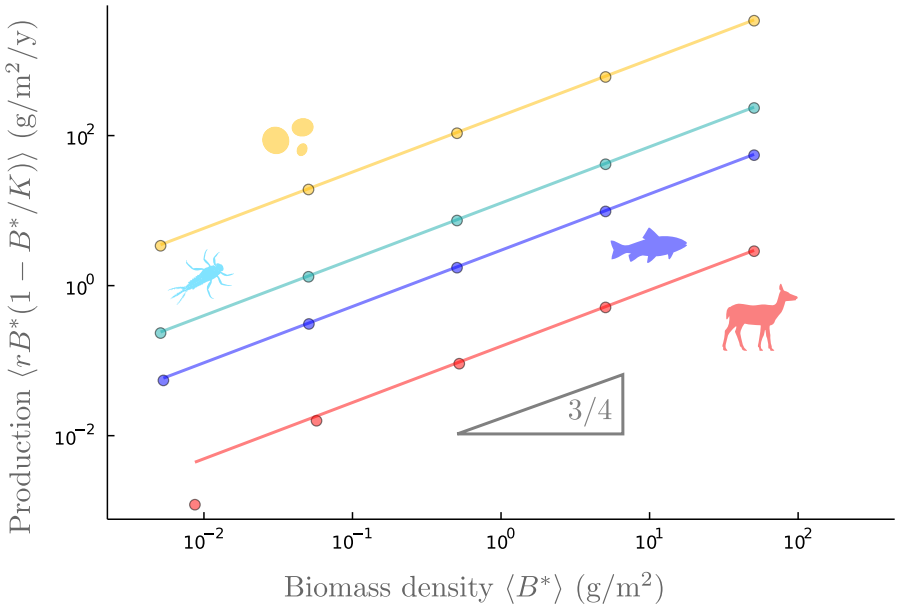

Figure 10: Average equilibrium production plotted versus average equilibrium biomass density. Each dot represents simulations for a community of $S = 50$ species, each color correspond to a specific difference between growth and mortality value: 437 yellow, 30 light blue, 7.05 blue and 0.37. The carrying capacity K is varied between 10^{-2} to 10^2 and we set the coefficient of variation $\sigma/\mu = 1$. The lines represent theoretical predictions from the cavity solution in Eq (98).

6.2 Macroecological patterns

We study here predictions and consistency checks of macroecological patterns for GLV under the assumptions used to recover production-biomass scaling.

6.2.1 Species abundance distribution

Consider a community with r extracted from a log-normal distribution, $\ln r \sim \mathcal{N}(\mu_r, \sigma_r)$, and for simplicity we cosnider $\sigma \to 0$. The cavity solution reads

$$B^* = K - \frac{\mu S K \langle B^* \rangle}{r} \,. \tag{99}$$

Following our assumptions $K = (r/b)^{1/(k-1)}$ and we have

$$B^* = (r/b)^{1/(k-1)} - \langle B^* \rangle \,, \tag{100}$$

therefore we have that, defining $\bar{B}^* := B^* + \langle B^* \rangle$,

$$\ln \bar{B}^* \sim \mathcal{N}(\mu_{\bar{B}^*}, \sigma_{\bar{B}^*}) \,, \tag{101}$$

with

$$\mu_{\bar{B}^*} = \frac{\ln b - \mu_r}{1-k}\,, \tag{102}$$

and

$$\sigma_{\bar{B}^*} = \frac{\sigma_r}{1-k}\,. \tag{103}$$

Therefore, as in the case of the sublinear model, we obtain a distribution for B^* four times wider than the one for r when $k = 3/4$.

6.2.2 Mean-variance scaling

In order to study the mean-variance scaling, we consider the variance of B^* which, from Eq. (96), reads

$$\langle (B^*)^2 \rangle - \langle B^* \rangle^2 = \frac{\sigma^2 K^2 S \langle (B^*)^2 \rangle}{r^2}\,. \tag{104}$$

Following our assumption we have $\sigma = \mu = r/KS$ and therefore we conclude that

$$\mathrm{var}(B^*) = \frac{\langle B^* \rangle^2}{S-1}\,. \tag{105}$$

6.2.3 Size-denisty scaling

Consistency with the size-density scaling is straightforward because within our assumption B^* does not depend on r, i.e. on the community type and ultimately on m. We have therefore

$$N^* = \frac{B^*}{m} \propto m^{-1}\,. \tag{106}$$

7 Back up sections

7.1 Generalized Lotka-Volterra with generic production

Maybe take out.

Consider a competitive community of S species defined by the following dynamics for the population abundances

$$\frac{dx_i}{dt} = g(x_i) - x_i \sum_{j \neq i} A_{ij} x_j \,, \tag{107}$$

where the A_{ij} are extracted from a distribution with mean $\mu > 0$ and standard deviation σ and the production term $g_i(x_i)$ may in principle include self-regulation terms which are only dependent on species i and parameters typical of species i.

If the equilibrium is feasible, denoting x_i^* the equilibrium values, we have

$$g_i(x_i^*) = x_i^* \sum_{j \neq i} A_{ij} x_j^* \,. \tag{108}$$

The jacobian evaluated at equilibrium is formally

$$J_{ij}\Big|_{\mathbf{x}=\mathbf{x}^*} = -x_i^* A_{ij} \,, \tag{109}$$

$$J_{ii}\Big|_{\mathbf{x}=\mathbf{x}^*} = g_i'(x_i^*) - \frac{g_i(x_i^*)}{x_i^*} \,, \tag{110}$$

where $g_i'(x_i^*)$ stands for $|dg_i(x_i)/dx_i|_{x_i=x_i^*}$ and we used the equilibrium relation.

In order to make some analytical progress let us focus on the case of uniform interactions ($\sigma \to 0$) and production with same parameters for every species, i.e. $g_i = g \ \forall i$. Then every species have the same equilibrium value $x_i^* = x^* \ \forall i$ and we can write down the equilibrium relation

$$g(x^*) = (S-1)\mu (x^*)^2 \,, \tag{111}$$

and the jacobian at equilibrium

$$J_{ij}\Big|_{x=x^*} = -x^* \mu \,, \tag{112}$$

$$J_{ii}\Big|_{x=x^*} = g'(x^*) - \frac{g(x^*)}{x^*} \,. \tag{113}$$

The largest eigenvalue correspond to

$$\lambda_{\max} = J_{ii}\Big|_{x=x^*} - J_{ij}\Big|_{x=x^*} \,, \tag{114}$$

therefore the stability condition reads

$$g'(x^*) - \frac{g(x^*)}{x^*} + x^* \mu < 0 \,. \tag{115}$$

By exploiting the equilibrium relation we can recast the last inequality as

$$g'(x^*) - \frac{g(x^*)}{x^*} + \frac{g(x^*)}{x^*(S-1)} < 0 \,, \tag{116}$$

therefore giving the general formal stability condition in terms of production at equilibrium and equilibrium density

$$g'(x^*) < \frac{g(x^*)}{x^*}\left(1 - \frac{1}{S-1}\right), \tag{117}$$

which for $S \to \infty$ can be approximated by

$$g'(x^*) < \frac{g(x^*)}{x^*}. \tag{118}$$

This last stability condition is quite general and, exploiting the trivial identity $1 = dx/dx|_{x=x^*} =: (x^*)'$, it can be written as

$$\frac{g'(x^*)}{g(x^*)} < \frac{(x^*)'}{x^*}, \tag{119}$$

which means that the relative change in growth should be less than the relative change in abundance itself.

Logistic and sublinear cases are recovered by substitutig resepctively $g(x) = x(1 - x/K)$ and $g(x) = x^k$.

References

[1] Guy Bunin. Ecological communities with Lotka-Volterra dynamics. *Physical Review E*, 95(4):042414, apr 2017.

[2] Matthieu Barbier, Jean-François Arnoldi, Guy Bunin, and Michel Loreau. Generic assembly patterns in complex ecological communities. *Proceedings of the National Academy of Sciences*, 115(9):2156–2161, 2018.

[3] Matthieu Barbier and Jean-François Arnoldi. The cavity method for community ecology. *bioRxiv*, 2017.

[4] Madhu Advani, Guy Bunin, and Pankaj Mehta. Statistical physics of community ecology: a cavity solution to MacArthur's consumer resource model. *Journal of Statistical Mechanics: Theory and Experiment*, 2018(3):033406, mar 2018.

[5] Wenping Cui, Robert Marsland Iii, and Pankaj Mehta. Effect of Resource Dynamics on Species Packing in Diverse Ecosystems. *Physical Review Letters*, 125, 2020.

[6] F. Roy, G. Biroli, G. Bunin, and C. Cammarota. Numerical implementation of dynamical mean field theory for disordered systems: application to the Lotka–Volterra model of ecosystems. *Journal of Physics A: Mathematical and Theoretical*, 52(48):484001, nov 2019.

[7] Ian A. Hatton, Andy P. Dobson, David Storch, Eric D. Galbraith, and Michel Loreau. Linking scaling laws across eukaryotes. *Proceedings of the National Academy of Sciences of the United States of America*, 116(43):21616–21622, oct 2019.

[8] Matthieu Barbier, Laurie Wojcik, and Michel Loreau. A macro-ecological approach to predation density-dependence. *Oikos*, 130(4):553–570, apr 2021.